Self-Passivation of Polymer-Layered Silicate Nanocomposites

Hao Fong,[†] Richard A. Vaia,*[,‡] Jeffrey H. Sanders,[‡] Derek Lincoln,[‡] Andrew J. Vreugdenhil,[§] Weidong Liu,[⊥] John Bultman,[§] and Chenggang Chen[§]

Universal Technology Corporation, Systran Federal Corporation, Air Force Research Laboratory, 2941 P. St., Room 136, Wright-Patterson Air Force Base, Ohio 45433-7750, and University of Dayton Research Institute, 300 College Park Ave., Dayton, Ohio 45469

Received February 21, 2001. Revised Manuscript Received July 30, 2001

Nanoscale dispersion of only a few weight percentage of layered silicate (montmorillonite) in nylon 6 and epoxy results in the formation of a uniform passivating and self-healing inorganic surface region upon exposure to oxygen plasma. The enrichment of inorganic is compositionally graded with respect to the surface and is due to the preferential oxidation of the polymer from the nanocomposite and the corresponding enhancement of the nanoscale layered silicate on the surface. The structure of the inorganic region is turbostratic, with an average distance between layered silicates of 1−4 nm. This ceramic-like silicate layer provides an overcoat to the nanocomposite and can significantly retard the penetration of oxygen plasma. Thus, layered silicate containing nanocomposites may enhance the survivability of polymeric materials in aggressive oxidative environments, such as atomic oxygen in low earth orbit (LEO). The formed inorganic region was characterized chemically and morphologically by X-ray photoelectron spectroscopy (XPS), attenuated total reflection infrared (ATR), transmission electron microscopy (TEM), and X-ray scattering.

Introduction

The combination of the U. S. Air Force's strong commitment to space, NASA's continued programs for space exploration, and rapidly increasing commercial satellite production has resulted in an urgent need for new lightweight, space-resistant materials with extended lifetimes. Unfortunately, aggressive environments encountered in orbit[1] have continually challenged the integrity of high-performance materials, especially carbon-based ones. Reported space environment damage to man-made bodies in orbit is staggering on the basis of numerous studies, such as those from STS missions and NASA's Long Duration Exposure Facility, which report that both radiation (atomic oxygen, vacuum ultraviolet, proton, electron and particle) and thermal cycling contribute to material degradation.[2,3] This drastically reduces the lifetime of the orbiting body.

Polymers are very attractive and desirable for use in space applications, in particular to reduce weight and enable multifunctional requirements. However, degradation is a prominent concern. Numerous approaches, based on deposition of an inorganic coating on the polymer surface or enrichment of inorganic precursors at the polymer surface in response to exposure to the aggressive space environment, have been demonstrated, with varying degrees of successes. The vast majority of these efforts have focused on polymer durability in low earth orbit (LEO), where atomic oxygen flux is very high ($\sim 10^{15}$ atoms/cm^2 s for orbital speed of 8 km/s[1,2,4]). General material strategies for imparting durability to polymers include direct deposition of a ceramic coating; blending with inorganic polymers and micron-scale fillers;[5,6] or copolymerization with phosphezenes,[7] siloxanes, or silsesquioxanes.[8−10] Issues associated with these approaches include failure of the coating in service, decreased mechanical and optical properties associated with blending, formation of volatile degradation products, and increased cost associated with copolymerization of inorganic monomers.

Over the past decade, the utility of layered silicate nanoparticles as additives to enhance polymer perfor-

[†] Universal Technology Corp.
[‡] Air Force Research Laboratory.
[§] University of Dayton Research Institute.
[⊥] Systran Federal Corp.

(1) Champion, K. S. W.; Cole, A. E.; Kantor, A. J. In *Handbook of Geophysics and the Space Environment*; Jursa, A. S., Ed.; Air Force Geophysics Lab., U. S. Air Force, National Technical Information Service: Springfield, VA, 1985; pp 14−1.
(2) Koontz, S. L.; Leger, L. J.; Visentine, J. T.; Hunton, D. E.; Cross, J. B.; Hakes, C. L. *J. Spacecraft Rockets* **1995**, *32*, 483.
(3) deGoh, K. K.; Banks, B. A. *J. Spacecraft Rockets* **1994**, *31*, 656.
(4) Tribble, A. S. *The Space Environment, Implications for Spacecraft Design*; Princeton University Press: Princeton, NJ, 1995.
(5) Mark, J. E., Lee, C. Y.; Bianconi, P. A. *Hybrid Organic−Inorganic Composites*; ACS Symposium Series 585; American Chemical Society: Washington DC, 1995.
(6) Thorne, J. A.; Whipple, C. L. In *The Effects of the Space Environment on Materials*; Society of Areospace Material and Process Engineers: North Hollywood, CA, 1967; p 243.
(7) Dang, T. D.; Thiesing, N. C.; Feld, W. A.; Cerbus, C. A.; Arnold, F. E. *Polym. Prepr.* **2000**, *41* (2), 1213.
(8) Gilman, J. W.; Schlitzer, D. S.; Lichtenhan, J. D. *J. Appl. Polym. Sci.* **1996**, *60* (4), 591.
(9) Gonzalez, R. I.; Phillips, S. H.; Hoflund, G. B. *J. Spacecraft Rockets* **2000**, *37* (4), 463.
(10) Zimcik, D. G.; Wertheimer, M. R.; Balmain, K. B.; Tennyson, R. C. *J. Spacecraft Rockets* **1991**, *28*, 352.

10.1021/cm010150o CCC: $20.00
Published on Web 09/13/2001

mance has been established.[11−14] These nanoscale fillers result in physical behavior that is dramatically different from that observed for conventional microscale counterparts. For instance, increased moduli,[15] increased strength, decreased permeability,[16,17] and reduced coefficient of thermal expansion[18] are observed with addition of only a few percent of exfoliated layered silicate, thus maintaining polymeric processability, cost, and clarity.

Recent studies of the ablation behavior of these polymer-layered silicate (PLS) nanocomposites demonstrated that the nanoscale dispersion of aluminosilicate layers enabled the formation of a tough inorganic passivation layer upon exposure to a thermal oxidative environment, decreasing the erosion rate relative to pristine resin by more than an order of magnitude.[19] The self-passivation response of PLS nanocomposites, containing only 1−7.5 vol % aluminosilicate, fundamentally derive from the high areal density of the inorganic, arising from the nanoscale dispersion of high aspect ratio plates. Enhanced durability, combined with improved mechanicals, reduced coefficient of thermal expansion, and enhanced barrier properties, affords unique opportunities for PLS nanocomposites in space systems.

Herein, the generality of the self-passivation response of nanocomposites to aggressive oxidative environments is examined for nylon 6 and epoxy nanocomposites within oxygen plasma. Oxygen plasma is an extremely strong oxidant and exposure to it provides an initial approximation to the performance of these materials in the complex oxidative environment of LEO.[4] The dispersion of only a few percent by weight of montmorillonite in the polymer results in the formation of a uniform passivation layer upon exposure to the plasma. This self-passivation layer retards penetration of the plasma and prevents further polymer degradation. Thus, polymer nanocomposite concepts, irrespective of the parent resin, are anticipated to enhance the survivability of polymeric materials in aggressive oxidative environments, such as against atomic oxygen in LEO. Furthermore, combination of a polymer nanocomposite with a purposeful plasma treatment to self-generate an inorganic-rich surface layer may provide functionally graded films with enhanced durability and barrier properties.

Experimental Section

Materials. Nylon 6/layered silicate (montmorillonite) nanocomposites with different percent layered silicate were received from Southern Clay Products, Inc. in the form of extruded films. Fabrication details can be found in refs 19 and 20. Additionally, solution cast films from 1,1,1,3,3,3-hexa-fluoro-2-propanol (use as received from Aldrich) solution and thermocompressed films (compressed at 230 °C, 2000 psi, using 10 layers of as-received films) were prepared. Morphological characterizations indicate that the montmorillonite in these nylon 6 systems is extensively exfoliated.[19,20]

Fabrication details for the epoxy/montmorillonite nanocomposites can be found in refs 21 and 22. Two organically modified montmorillonites, SC16 [Closite Na^+ (CEC $\sim$ 92 mequiv/100 g, Southern Clay Products, Inc.] with hexadecylammonium hydrogen chloride) and I.30E (Nanocore, Inc., CEC$\sim$145 meq/100 g, octadecylammonium hydrogen chloride), were used to make epoxy (Epon862/Cure Agent W, Shell) nanocomposites. Morphological characterizations of theses and related epoxy systems indicate that the montmorillonite dispersion is in general mixed, consisting of individual exfoliated layers, highly swollen crystallites (>10 nm layer spacing), and clusters of 2−3 intercalated layers (<6 nm layer spacing).[21,22]

Processing. Oxygen plasma was generated using a GSC-200 plasma generator (March Instruments, Inc. Concord, CA) Oxygen plasma concentration was approximately 10^{18} ions (or radical) per liter.

Characterization. X-ray photoelectron spectroscopy (XPS) spectra were recorded using a Surface Science Instrument SSX-100. This system produces monochromatic Al Kα X-ray radiation with energy of 1486.6 eV. This instrument was operated using a 300 μm X-ray spot for all experiments. Attenuated total reflection infrared (ATR) spectra were obtained on a Bruker Equinox 55 FT-IR spectrometer using a SpectraTech Model 300 ATR. By varying the types of crystals and the angles of incidence, information from different depths within the sample can be obtained.

The transmission electron microscope (TEM) employed in the work was a Philips CM-200 TEM with a LaB_6 filament operating at 200 kV. For TEM, nanocomposites before and after the plasma treatment were embedded in epoxy, and 50−70 nm thick sections were microtomed at room temperature using a Reichert-Jung Ultracut Microtome and mounted on 200 mesh copper grids.

X-ray diffraction measurements were carried out with a rotating anode X-ray generator (RU-200BH, Rigaku-Rotaflex, 20 KV, 50 mA) with Cu Kα radiation (λ = 1.54 Å). A pinhole (1 mm) collimation positive-sensitive detector at 0.75 m from the sample was used for data collection. Silver Behenate standard was used for 2θ calibration.

Oxygen plasma erosion rates were determined by measuring the weight loss upon treatment. Weight changes could also be converted to thickness changes, since the total surface areas of the treated samples were easily measured.

Results and Discussion

Oxygen plasma is an extremely strong oxidant, containing many species including free radicals, cations, anions, electrons, ozone molecules, and electrons. Polymers and other organics are, by far, among the most vulnerable materials when exposed to oxygen plasma. Generally, unfilled materials containing only C, H, O, N, and S react with approximately the same efficiency, or volume loss per atom, of (1−4) $\times$ 10^{-24} cm^3/atom.[23]

(11) Alexandre, M.; Dubois, P. *Mater. Sci. Eng.* **2000**, *28*, 1−63.
(12) Vaia, R. A. In *Polymer Clay Nanocomposite*; Pinniavaia, T. J., Beall, G. W., Eds.; John Wiley & Sons: New York, 2000.
(13) Collister, J. In *Polymer Nanocomosites*; Vaia, R. A., Krishnamoorh, R., Eds.; American Chemical Society: Washington DC, 2001.
(14) Messersmith, P.; Giannelis, E. P. *J. Polym. Sci. A: Polym. Chem.* 1995, *33*, 1047. Messersmith, P.; Giannelis, E. P. *Chem. Mater.* **1994**, *6*, 1719. Lan, T.; Pinnavaia, T. J. *Chem. Mater.* **1994**, *6*, 2216. Lan, T.; Pinnavaia, T. J. *Chem. Mater.* **1994**, *6*, 573 1994. Lan, T.; Pinnavaia, T. J. *Chem. Mater.* **1995**, *7*, 2144. Wang, Z.; Pinnavaia, T. J. *Chem. Mater.* **1998**, *10*, 1820. Massam, J.; Pinnavaia, T. J. *Mater. Res. Soc. Symp. Proc.* **1998**, *520*, 223. Vaia, R. A.; Brown, J.; Curliss, D. *Chem. Mater.* **2000**, *12* (11), 3376.
(15) Messersmith, P. B.; Giannelis, E. P. *Chem. Mater.* **1994**, *6*, 1719.
(16) Messersmith, P. B.; Giannelis, E. P. *J. Polym. Sci.: Part A: Polym. Chem.* **1995**, *33*, 1047.
(17) Scherer, C. Proceedings of the New Plastics '99. London, 1999. Yano, K.; Usuki, A.; Okada, A. *J. Polym. Sci. A: Polym. Chem.* **1997**, *35*, 2289.
(18) Kojima, Y.; Usuki, A.; Kawasumi, M.; Okada, O.; Fukushima, Y.; Kujima, Y.; Kamigraito, O. *J. Mater. Res.* **1993**, *8*, 1185.
(19) Vaia, R. A.; Price, G. P.; Ruth, P. W.; Wguyen, H. T. *J. Appl. Clay Sci.* **1999**, *15*, 67.
(20) Lincoln, D. M.; Vaia, R. A.; Wang, Z.-G.; Hsiao, B. S. *Polymer* **2001**, *42*, 1621. Cho, J. W.; Paul, D. R. *Polymer* **2001**, *42*, 1083.
(21) Chen, C. G.; Curliss, D. SAPME 2001, May 6−10, 2001, Long Beach, CA.
(22) Brown, J. M.; Curliss, D.; Vaia, R. A. *Chem. Mater.* **2000**, *12*, 3376.

Thus, direct exposure of polymers to oxygen plasma leads to rapid degradation and removal of organic material and is thus commonly used to clean surfaces and as a reactive ion etch in microfabrication. However an aggressive plasma environment is also commonly used to deposit coatings or chemically modify polymer surfaces.[24−26] Chemistry far from equilibrium in plasma offers access to materials that cannot be made by other synthesis routes. For instance, Clarson and co-workers reported the use of plasma-enhanced chemical vapor deposition to deposit thin barrier layers of hexamethyldisiloxane as a possible methodology to limit or eliminate diffusion of chromophores across interfaces in optical stacks;[25] LeBras et al. reported dramatic improvement of fire retardancy and thermal stability of polymer films coated by organosilicon films using a cold remote plasma;[27] and Thomas and co-workers demonstrated the possibility to synthesize essentially automatically flat amorphous SiO_2 thin films with a low residual carbon contamination (below 1 atom %) from poly(pentamethyldisilylstyrene) by exposure to UV irradiation in a flow of O_2.[26] Paralleling the products that result from chemistry in plasmas and drawing from the preferential removal of organics, polymer−inorganic nanocomposites in plasma environments offer unique possibilities to create functionally graded materials and self-passivating systems.

Figure 1 summarizes the effect of oxygen plasma exposure to pure nylon 6 and nylon 6 nanocomposite containing 7.5 wt % montmorillonite (recast samples, ∼100 μm thick). In contrast to the almost complete deterioration of the pristine polymer after 8 h (480 min) of continuous exposure, the erosion of the nanocomposite was minimal, with no significant decrease in thickness. The buckling of the nanocomposite after exposure probably arises from differences in thermal expansivity of the self-generating ceramic surface and the bulk polymer nanocomposite.

As-received, melt extruded films of the nylon 6/layered silicate nanocomposite (7.5 wt %) develop of a colorful, interferometic surface reflection upon exposure to oxygen plasma for 1 h. The optical interference effects suggest the alteration of the surface composition is highly uniform and on the order of 500 nm.

Figure 2 summarizes the oxygen plasma erosion rates of neat nylon 6 and nylon 6 nanocomposites with 5.0 and 7.5 wt % montmorillonite (recast samples, ∼100 μm). The long time, equilibrium erosion rates decrease with increased concentration of montmorillonite (60, 15, and 10 nm/min for nylon 6, nylon 6/5.0 wt % montmorillonite nanocomposite, and nylon 6/7.5 wt % montmorillonite nanocomposite, respectively). In contrast, the intial erosion rate of the prisitine polymer and the nanocomposites are comparable (>150 nm/min). This implies that initially the oxygen plasma removes organic material from the surfaces irrespective of the nanostructure. However, as the organic is removed, the inorganic concentratrion in the near surface region increases and the effective erosion rate decreases. This transition is dependent on the concentraion of layered silicate in the nanocomposite, decreasing with increased concentration of montmorillonite (120 min for nylon 6/5.0 wt % montmorillonite nanocomposite and 60 min for nylon 6/7.5 wt % montmorillonite nanocomposite). The effect of this self-generating passivation layer is to decrease erosion rate and increase lifetime, by greater than an order of magnitude (∼15 times)! Note that

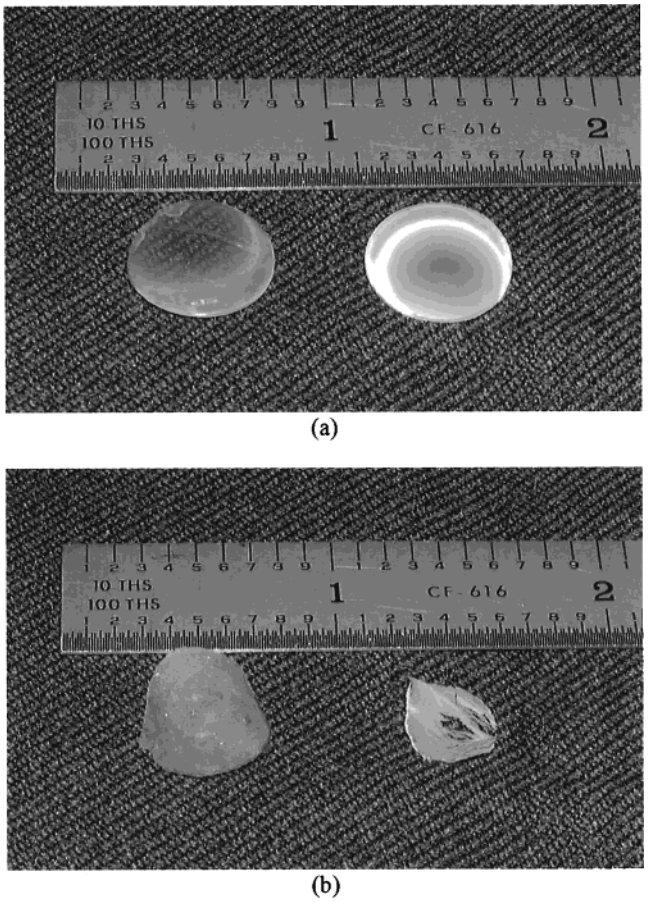

Figure 1. Nylon 6/layered silicate nanocomposite (left in both pictures) and neat nylon 6 (right in both pictures) before (a) and after (b) plasma treatment for 8 h.

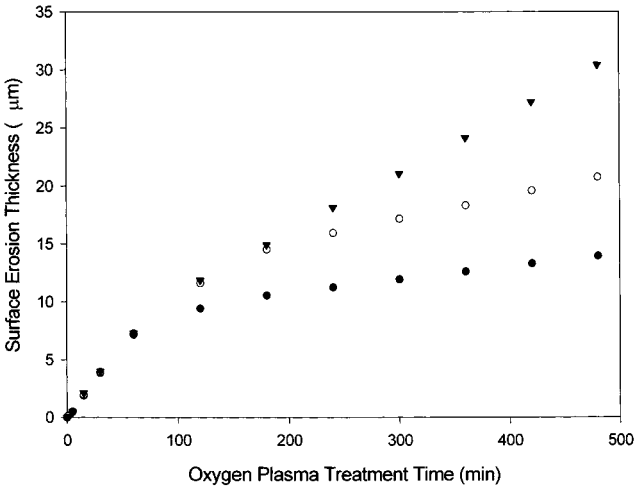

Figure 2. Oxygen plasma surface erosion rate of neat nylon 6 (▼), nylon 6/5.0 wt % layered silicate nanocomposite (○), and nylon 6/7.5 wt % layered silicate nanocomposite (●).

(23) Reddy, R. M. *J. Mater. Sci.* **1995**, *30*, 281.
(24) Haaland, P. D.; Clarson, S. J. *Trends Polym. Sci.* **1993**, *1* (2), 40.
(25) Johnson, E. M.; Clarson, S. J.; Jiang, H.; Su, W.; Grant, J. T.; Bunning, T. J. *Polymer* In press.
(26) Brinkmann, M.; Chan, V.; Thomas, E. *Chem. Mater.* In press.
(27) Jama, C.; Quede, A.; Le Bras, M. *ACS Polym. Mater. Sci. Eng.* **2000**, *August*, 75.

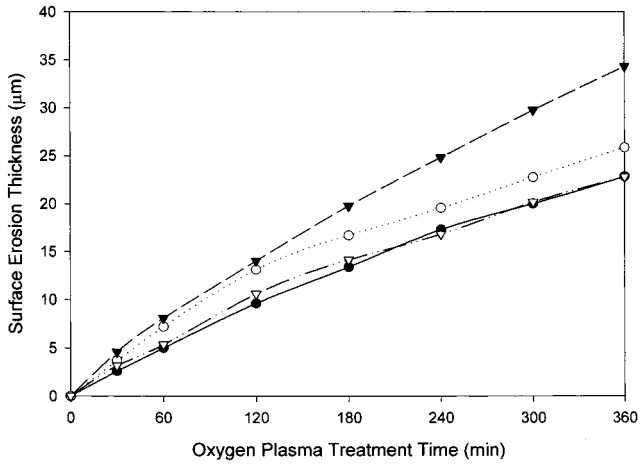

Figure 3. Oxygen plasma surface erosion rate of neat epoxy (▼), epoxy/3.0 wt % SC16 (○), epoxy/6.0 wt % SC16 (●), and epoxy/6.0 wt % I30 nanocomposites (▽).

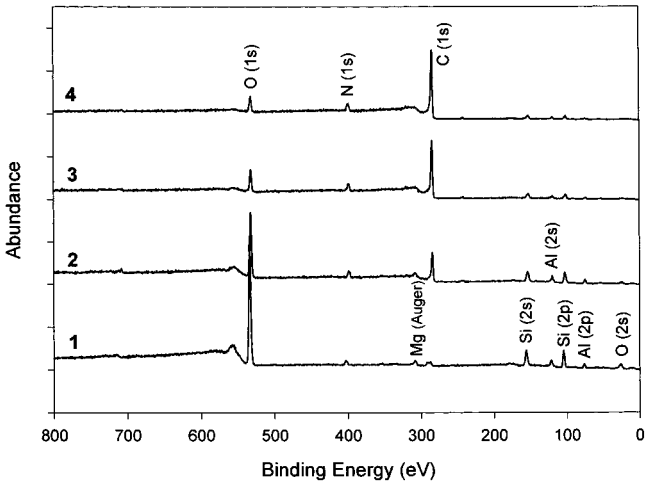

Figure 4. XPS characterization of the inorganic layer formed on the surface of the nylon 6/7.5 wt % layered silicate nanocomposite before and after oxygen plasma exposure for 1 h: (1) exposed film before argon ion etching, (2) exposed film after argon ion etching for 20 min, (3) exposed film after argon ion etching for 40 min, and (4) unexposed film.

although the formation of an inorganic passivation layer cannot occur for pure nylon 6, creation of carbonaceous char is also able to provide modest protection, as indicated by the decrease in erosion rate around 120 min.

Similar behavior is also observed from epoxy nanocomposites. Figure 3 shows the surface erosion of epoxy nanocomposites after oxygen plasma treatment. As observed from the nylon 6 nanocomposites, the incorporation of dispersed organically modified montmorillonite (SC16 or I.30) also retards the erosion rates. The retardation effect of 6 wt % reinforced nanocomposite is greater than 3 wt %, with no significant difference of the retardation between the two different organically modified montmorillonites. As with the nylon 6 nanocomposites, two regimes occur, characterized by an initial erosion rate and a long-time equilibrium erosion rate. In contrast though, the initial erosion rate for the epoxy system decreases with increased weight percentage of montmorillonite. Overall, the retardation effect for these epoxy nanocomposites is not as great as that in the nylon 6 nanocomposites. A possible factor may be assocaited with the different morphologies. Previous transmisson electron microscopy by Vaia[19−22] and Chen[21] indicates that the layer exfoliation in the epoxies is not as extensive as in nylon 6. Additionally, elongation and shear flow in melt extrusion and injection molding or slow solvent removal in solution cast films have been shown to enhance alignment of the layers parrellel to the surface of nylon 6 nanocomposite films and pellets.[19,28,29] The preferential alignment will maximize the areal density of the inorganic parallel to the exposed surface, enhancing the rate of inorganic enrichment relative to organic removal.

A detailed understanding of the formation of the passivation layer necessitates detailed compositional analysis and morphology studies.

Composition. Figure 4 summarizes XPS spectra at various depths within an extruded nylon 6 nanocomposite film after 1 h of oxygen plasma treatment. Ar^+ ion etching was used to remove material to examine the relative composition within the film. Note that calibration of the etch time to an etch depth is difficult for these heterogeneous systems, and thus changes in chemical composition is discussed relative to the surface.[30]

With respect to a nanocomposite film before plasma exposure, the chemical composition of the nanocomposite surface after exposure to oxygen plasma is carbon-deficient and inorganic-rich. This suggests that very little polymer remains at the surface of the film. Etching into the film reveals increasing amounts of carbon and decreasing amounts of Si, Al, Mg, and O, indicating an increased concentration of polymeric material. After Ar^+ ion etching for 40 min, the complete XPS spectrum (Figure 4, curve 3) is very similar to that of the nanocomposite prior to exposure to oxygen plasma (Figure 4, curve 4), indicating that the composition changes associated with the oxygen plasma are confined to the near-surface region of the nanocomposite. Comparable examination of nylon 6 nanocomposite prior to exposure to oxygen plasma shows no compositional variation perpendicular to the surface, with the XPS spectra similar to curve 4 for all Ar^+ etching times.

Figure 5 shows the relative chemical compositions derived while the XPS spectra were monitored during continuous Ar^+ etching the film. Note that the atomic percent composition in Figure 5 is based on the five most abundant elements (Si, Al, C, O, and N) only—hydrogen and other elements have been neglected. Detailed depth profiling reveals three distinct regions: (i) surface region (i.e., within 500 s of etching time), containing high concentration of Si, Al, Mg, and O and very little carbon; (ii) transition region (i.e., 500−3000 s of etching time), containing increasing amounts of carbon and decreasing amounts Si, Al, Mg, and O with increased depth; and (iii) bulk region (i.e., longer than 3000 s of etching time),

(28) Kojima, Y.; Usuki, A.; Kawasumi, M.; Okaua, A.; Kurachi, T.; Kamigaito, O.; Kaji, K. *J. Polym. Sci., Part B, Polym. Phys.* **1995**, *33*, 1039.

(29) Kojima, Y.; Usuki, A.; Kawsumi, M.; Okaua, A.; Kurauchi, T.; Kamigaito, O.; Kaji, K. *J. Polym. Sci., Part B, Polym. Phys.* **1994**, *32*, 625.

(30) The Ar^+ etching rate of organic and inorganic material is anticipated to be different, which results in preferential removal of organic and enrichment of inorganic with etch depth; thus compromising the absolute determination of elemental composition with depth.

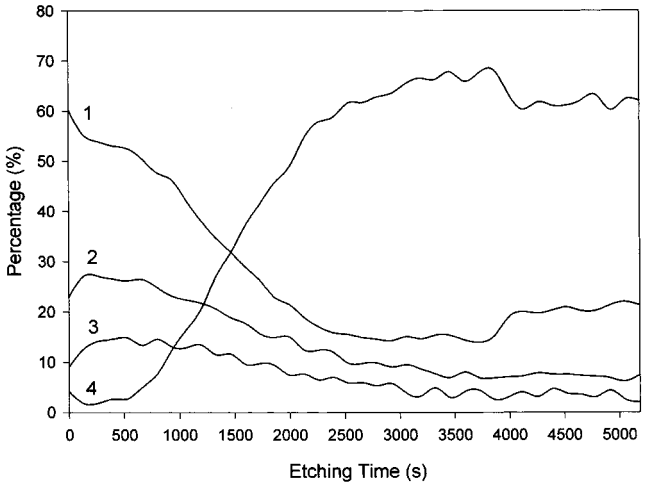

Figure 5. Relative elemental profile for Ar^+ ion etching of nylon 6/7.5 wt % layered silicate nanocomposites after 1 h of plasma exposure: (1) oxygen, (2) silicon, (3) aluminum, and (4) carbon.

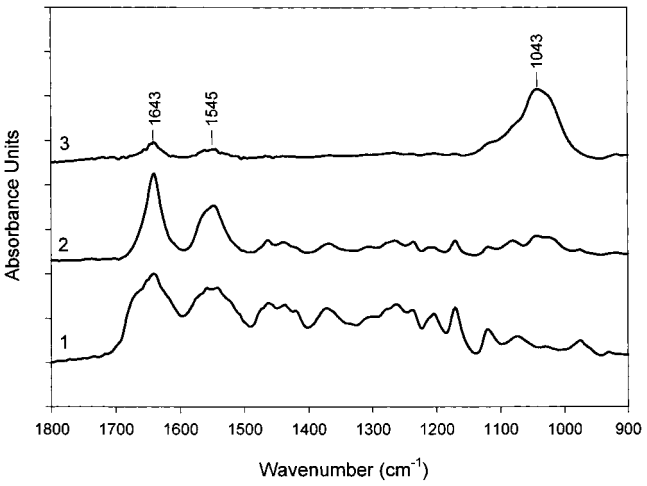

Figure 6. Attenuated total reflection (ATR) spectra (0.65 μm depth): (1) neat nylon 6, (2) nylon 6/7.5 wt % layered silicate nanocomposite, and (3) nylon 6/7.5 wt % layered silicate nanocomposite after 1 h of plasma treatment.

largely unaffected by the oxygen plasma and corresponding to the original composition of the nanocomposite. Before Ar^+ etching (pristine film surface, etching time = 0 s), the slight increased percentage of carbon and oxygen is due to the surface adsorption of carbon dioxide and other carbon-containing compounds. In the transition region, the formation of a carbonaceous tar may enhance the carbon percentage relative to the unexposed and bulk (etching time > 3750 s) nanocomposite.

The ratio of Si:Al:O at the very surface of the exposed nylon 6 nanocomposite is 22.96%:9.14%:60.2%, which is 2.5:1:6.5. This ratio corresponds well to that generally anticipated from low-magnesium montmorillonite [2.3:1:6.8, $(Al_{3.5}Mg_{0.5})Si_8O_{20}(OH)_4$[11]]. This further indicates that a thin layer of aluminosilicate covers the surface of the oxygen plasma treated nanocomposite film. Detailed identification of inorganic species is under investigation.

ATR provides additional details of the plasma treated nanocomposites. Figure 6 shows the ATR spectra from the top 0.65 μm of neat nylon 6 and nylon 6/7.5 wt % montmorillonite nanocomposites before and after 1 h of oxygen plasma treatment. The broad absorption at 1043 cm^{-1} is the result of Si−O−Si stretching motions (1000−1100 cm^{-1}). The peak at about 1643 cm^{-1} is due to the primary amide carbonyl absorption (1640 cm^{-1}), and the peak at 1545 cm^{-1} is associated with the hydrogen in the trans position to the carbonyl of nylon 6 (1540−1550 cm^{-1}).[31] Figure 6 indicates that the top 0.65 μm of the nylon 6 nanocomposite after plasma treatment contains minimal polymer, the majority being silicate.

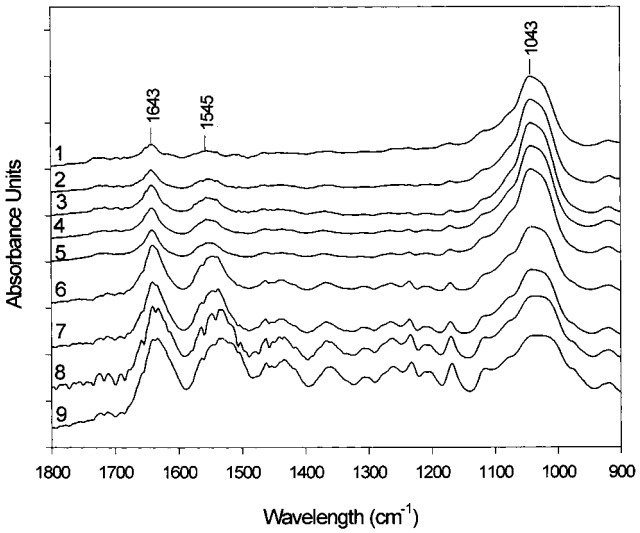

Figure 7. ATR of 1-h-treated nylon 6/7.5% layered silicate nanocomposites with different surface thicknesses: (1) 0.47 μm, (2) 0.5 μm, (3) 0.6 μm, (4) 0.7 μm, (5) 0.8 μm, (6) 1.0 μm, (7) 1.2 μm, (8) 1.4 μm, and (9) 1.6 μm.

By changing the incident angle and coupling crystal, ATR spectra reflecting the average composition for various depths relative to the surface can be obtained. Figure 7 summarizes these results for the nylon 6 nanocomposite after 1 h of oxygen plasma exposure. Each spectrum represents the average composition between the surface and the penetration depth. For instance, curve 6 presents the information from the topmost 1.0 μm layer. Note that the relative intensity of the vibrational absorptions within a spectrum reflects the relate composition within the layer. Direct comparison between spectra is only qualitative. As the infrared penetration depth increases, the average content of polymer increases. The region between the surface and 0.47 μm (curve 1) contains very little polymer, since the intensity of the peaks at 1643 and 1545 cm^{-1} is quite small. The transition of the inorganic layer to bulk material begins at a depth of several hundred nanometers, as reflected by the increasing relative intensity of the vibrations associated with nylon as the penetration depth increases. Beyond the depth of 1.0 μm, which is presented as curves 6−9, no significant changes of the relative intensities of the absorbencies are observed. Additionally, these spectra are identical with that obtained from the unexposed nanocomposite. This implies that the thickness of the inorganic layer is around 0.5−1.0 μm.

Morphology. Figures 8 shows the bright field transmission electron micrographs of the cross-section of

(31) Pouchert, C. J. *The Aldrich Library of Infrared Spectra*; Aldrich Chemical Co., Inc.: Milwaukee, WI, 1970.

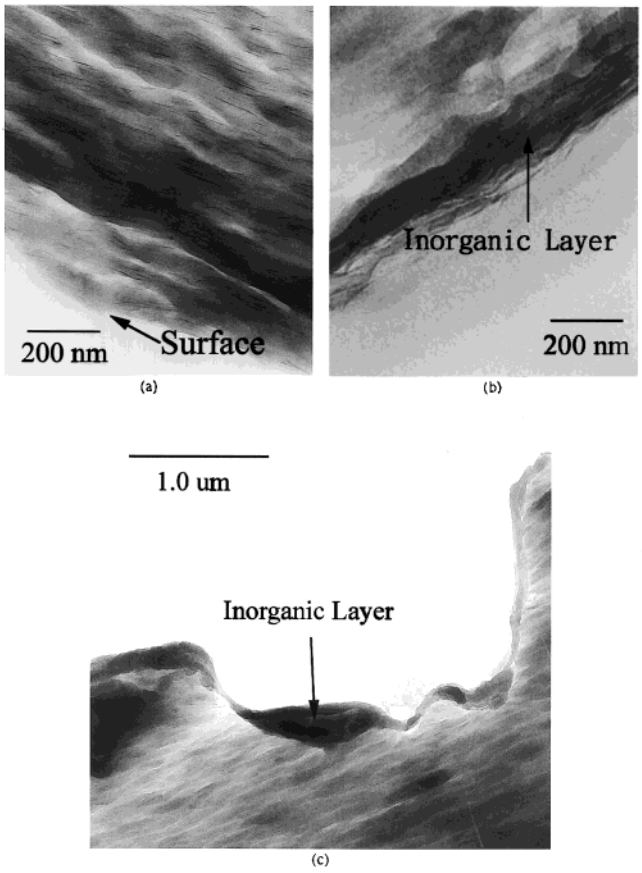

Figure 8. TEM images of nylon 6/7.5 wt % clay nanocomposites before (a) and after (b, c) 1 h of oxygen plasma treatment.

nylon 6/7.5 wt % montmorillonite nanocomposite before and after 1 h of oxygen plasma treatment. Consistent with those observed from previous studies,[19] the dark lines are individual silicate layers oriented perpendicular to the sample surface. The average dimensions of these layers are approximately 1 nm thick and tens to hundreds of nanometers long. Note that the lengths determined from the images are associated with the cross-section arising from microtoming and thus may not represent the true distribution in lateral size of the silicate layers.

After oxygen plasma treatment, the enhanced silicate at the surface is shown in Figure 8b. The enhanced silicate region varies from 0.1 to 0.5 μm thick, being well-aligned parallel to the surface. Additionally, the formation of the inorganic surface is conformal. Figure 8c shows a conformal inorganic coating within a surface dimple.

Studies of the microstructure within the inorganic layer were conducted using Bragg−Brentano X-ray diffraction and are summarized in Figure 9. In contrast to transmission (Laue) geometry, reflection (Bragg−Brentano) geometry at low scattering angles preferentially reflects the structure at the sample surface.[12] The abrupt increase in the intensity at $2\theta < 2.5$ is associated with Lorentz polarization, experimental geometry, and parasitic scattering from the sample holder.

The XRD curves of neat nylon 6 before and after 3 h of oxygen plasma treatment are identical; thus, only one curve is shown in Figure 9. The increase in the scattering intensity of the nanocomposite is associated with

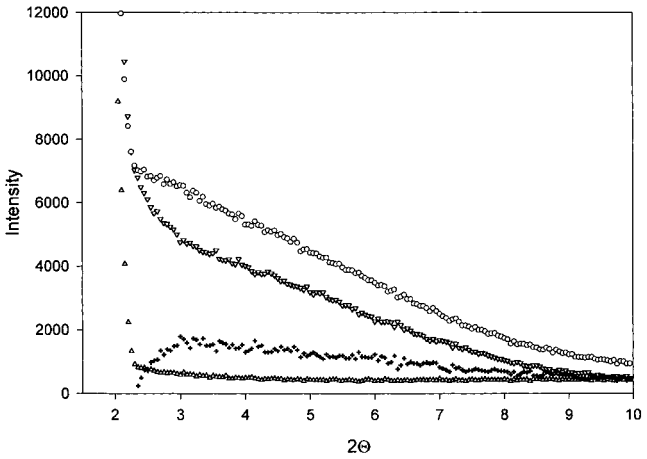

Figure 9. XRD of neat nylon 6 (△) and nylon 6/7.5 wt % layered silicate before (▽) and after (○) the oxygen plasma exposure. The difference between the scattering before and after oxygen plasma exposure is also included (+).

scattering from the silicate sheets.[12,32] The further increase in the scattering intensity after plasma treatment is due to the formation of the enriched silicate region on the surface. The change in shape of the scattering curve after oxygen plasma treatment indicates an enhancement of plate−plate correlations in the inorganic layer. Subtracting the scattering traces of the nanocomposite before oxygen plasma exposure from those after exposure reveals a broad peak with a large range of 2θ angles, indicating that the structure of the formed silicate layer is actually turbostratic with an average distance between layers of 1−4 nm. This agrees with qualitative observations from the TEM (Figure 8b,c). A turbostratic structure of decomposition char arising from the collapse of the originally exfoliated silicate morphology has been previously observed in flammability[32] and ablative[19] studies.

Conclusion

Polymer−layered silicate nanocomposites are able to self-generate a compositionally graded silicate passivation layer upon exposure to oxygen plasma. Results indicate that the thickness of the layer varies from a few hundred nanometers to 1 μm, and chemical composition of the uppermost region is almost completely inorganic and comparable to the base montmorillonite. The formation of the layer is due to the preferential oxidation of the polymer and the corresponding enrichment of the nanoscale layered silicate on the surface. The erosion profile of the nanocomposites shows an induction phase that is consistent with required oxidation of the polymer to form the passivation silicate layer. After the passivation layer is formed, the degradation of the underlying polymer can be significantly retarded, up to an order of magnitude. Since the formation of the passivation layer is an inherent property of the bulk nanocomposite, failure of the passivation layer in an aggressive environment will expose bulk nanocomposite, capable of re-forming the passivation region, so-called self-healing.

In general, nanocomposite concepts could enhance the survivability of polymeric materials against strong

(32) Gilman, J. W. *Appl. Clay Sci.* **1999**, *15*, 31.

oxidants, for instance, oxygen plasma, atomic oxygen, and ozone. Furthermore, the compositionally graded surface will be more durable to thermal cycling and mechanical flexure, which lead to failure in conventional rigid coatings on flexible substrates. In addition to enhancing survivability, combination of nanocomposite concepts to self-generate the inorganic surface will provide commercial films with enhanced durability and barrier properties before introduction to service.

Acknowledgment. The authors would like to thank Drs. Shawn Phillips, Peter J. John, Clifford A. Cerbus, and Hong G. Jeon for XPS, TEM work, and helpful discussion. This work was supported by Entrepreneurial Research of U.S. Air Force Office of Scientific Research. The authors are grateful to Southern Clay Products, for supplying the nylon 6/layered silicate nanocomposites.

CM010150O